CHEMICAL ENGINEERING TRANSACTIONS
VOL. 33, 2013
A publication of AIDIC
The Italian Association of Chemical Engineering
Online at: www.aidic.it/cet
Guest Editors: Enrico Zio, Piero Baraldi

ISBN 978-88-95608-24-2; **ISSN** 1974-9791
DOI: 10.3303/CET1333133

Analysis on Errors Generation in Torsional Angle Measurement of Marine Shaft by Phase Difference Method

Kun Yang*[,a], Xinping Yan[a], Xincong Zhou[a], Xiang Zheng[b], Songsong Liao[b]

[a]Reliability Engineering Institution, School of Energy and Power Engineering, Wuhan University of Technology, Heping Avenue, Wuhan, Hubei, 430063, China
[b]Shenzhen Yateks Optical Electronic Technology Co. Ltd, Cheonan Digital City, Longgang Section, Shenzhen, Guangzhou, 518057, China
kunyangwhut@163.com

The method based on phase difference for shaft power measurement is used widely and supposed to be more accurate than traditional methods, like by strain gauge. There are some potential errors which probably have great influence to experiment result when the torque of shaft is calculated according to torsional angle between two coding wheels. The sources of error are researched and analysed in four aspects. The first one is from the quantification error in FPGA (Field Programmable Gate Array), which is caused by the counter's frequency. Lower counter frequency may leads to bigger error. The research in this problem is to find out a quantification frequency that is accurate enough but won't increase too much the amount of data. The second one is temperature drift in sensor. It is generated by the variation of environment temperature. The influence of temperature is universal in application. The error tolerance and treatment of temperature drift are discussed in the research work. The third and fourth error sources in measurement are decentred error and perpendicularity error. Both of them are the result of inexactitude installation of coding wheels on shaft. All the sources of error discussed may introduce a lot of uncertainty to the continuous torque and power monitoring. So the tolerances of the potential errors and the extent of improvement are discussed after the analysis of error sources. The research work will help the engineers to understand the processing of error generation and prevent unnecessary problems in monitoring of shaft torque and power, especially the error that may result in the missing of important signals for fault diagnosis.

1. Introduction

Various methods were developed to measure and monitor the working condition of shaft in marine propulsion system. They mainly focus on the monitoring of torque, power, and torsion oscillation. These methods can be divided into contact and non-contact measurement. Strain gauge is widely used for a long time as a contact method in power and torsion oscillation measurement, like acoustic wire strain gauge (Drinkwater, 1966), and it is still being used in current measurement. Some other strain gauges based on strain foil were developed (Lonsdale et al. 1996; Li et al., 2010; Dai et al., 2007; Zhu et al., 2009), and it makes the measurement of shaft torque and power relatively easier. However, the contact measurement suffered from several fundamentally fatal defects, such as the problems of power supply, signal drifting with surrounding temperature, troublesome in strain gauge positioning and signal transmission. So the non-contact method is preferred and become popular to most of applications in nowadays.
The way to measure the twisted angle in high precision and stability is the key point to the monitoring of shaft status. Moore J, et al (1985) and Witte J (1991) developed two kinds of non-contact apparatus for measuring shaft torque. These two apparatuses are similar in basic structure but different sensors and method are used to calculate the torsion angle. Yu Chengbao, et al. (2005) proposed a method to mount an electromagnetic coil on shaft and the variation of magnetic field will induce electronic signal in another coil. The torsion can be worked out from the induced signal according to Faraday's law of electromagnetic induction. The coils in this method are big and hard to mount in measurement, and the metallic

surrounding of marine propulsion system can disturb the electromagnetic signal and introduce error to measurement. Gandarillas C, et al. (2003) invented a measurement structure based on magneto elastic non-compliant torque sensor to realize a non-contacting monitoring for rotatable shaft. N. Whitehead, et al. introduced metallic tuning-fork resonator into the measurement of torque (1999). The instrument structure is similar to vibrating-wire measurement (2008), and it is usually clumsy and unwieldy. This will bring trouble to installation and result in erroneous data. The Kongsberg Shaft Power Meter, called MetaPower system, measures torque and power transferred from the main engines to the propellers (Metapower, 2002). This method uses optical-fibers to transmit laser signal. And through the optical coding wheels on shaft, the laser signal is modulated to detect the torsion of shaft.

The error sources and tolerances of the non-contact method for shaft power and torque measurement are analysed in this paper. The purpose of the research work is to find out the influent factors that may bring trouble to the shaft torque measurement with the phase difference method, and to build up the relationship of these factors and the measurement error. Finally, some effective resolutions can be provided to the engineers to avoid the uncertainty in monitoring.

2. Calculation of Torsion Angle

The fundamental principle of shaft power measurement based on phase difference is that the two channels of pulse signal from position detectors can be quantified by a digital counter. There should be an initial bias angle between the opposite two teeth in the two coding wheels. It is the initial bias angle φ. The pulse signals are generated by the teeth of coding wheel while scanning through the optoelectronic sensors. Suppose the counter frequency is f, and the central angle of every vane in coding wheel is Φ. These two parameters are available in designing. T in Figure 1 is relative to Φ, so the quantification of T means the quantification of Φ. A higher counter frequency F might be used to quantify the initial bias angle φ and its variation Δφ (torsional angle). It results in t and Δt in Figure 1. Because the numerical relationship between f and F is known, the initial bias angle φ and torsion angle Δφ that are related to t and Δt can be calculated. Therefore, φ and Δφ can be derived from following equations (1) and (2) (suppose the numerical relationship between f and F is F = nf, and the quantified values of T, t and Δt are A, a and Δa).

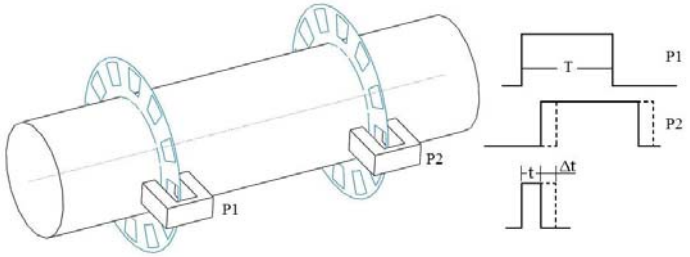

Figure 1: Diagram of waveforms from position detectors and phase difference

$$\varphi = \frac{n\Phi a}{A} \tag{1}$$

$$\Delta\varphi = \frac{n\Phi \Delta a}{A} \tag{2}$$

3. Analysis on the sources of error

3.1 Quantification error in FPGA

Eight counter frequencies were used to test the quantification system and verify the validation of this method. The original counter clock input is generated by a 40MHz crystal oscillator. The lowest counter frequency is output from 10th bit of counter, which is used for frequency division. So the lowest counter frequency is 40MHz/1024 = 39.062 kHz as shown in Table 1. And all the other counter frequencies are 2^m times of the lowest one. The m is a value between 0 and 7. The width of a sample square signal is about 0.2816ms. Two groups of data were acquired in experiment. The first group contains 100 pulse width data points under every counting frequency, and in the second one, 200 data were acquired under every counting frequency. The purpose of this experiment is to see the trend of quantification errors and their influent factors. The theoretical pulse widths and the relative errors of average pulse width in two data group are shown in Table 1.

Table 1. Experimental Result for Different Counter Frequency

Counting Frequency(kHz)	Theoretical Quantified Value	Experiment Result of 1st Group	Relative Error of 1st Group	Experiment Result of 2nd Group	Relative Error of 2nd Group
39.062	11	10.82	0.016364	10.83	0.015455
78.125	22	21.71	0.013182	21.735	0.012045
156.25	44	43.37	0.014318	43.475	0.011932
312.5	88	86.83	0.013295	86.79	0.01375
625	176	173.61	0.01358	173.65	0.013352
1250	352	347.23	0.013551	347.215	0.013594
2500	704	694.54	0.013438	694.49	0.013509
5000	1408	1388.95	0.01353	1388.96	0.013523

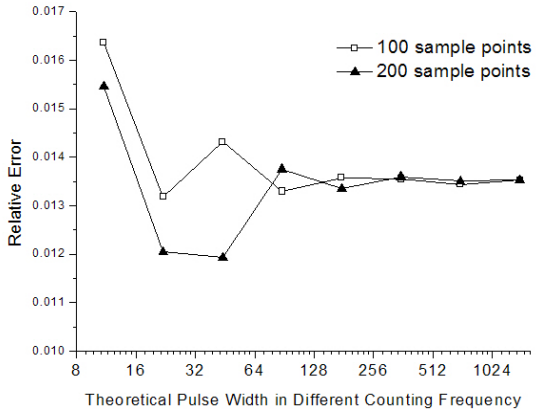

Figure 2: The variation of relative errors in different sample points

The theoretical pulse width is calculated according to measured value in lowest counting frequency of the eight ones. This quantified value vibrates between 10 and 11. We evaluate the potential influence to analysis result by choosing different theoretical value, and recognized that it is the same thing when choose 10 or 11 as theoretical value. The relative error of average pulse width data in each counting frequency can be used to analyse the two groups of sampled data to find out the characteristics of the quantification system. In Figure 2, the x-axis is frequency and y-axis is value of relative error. The x-axis is a log axis because all the theoretical pulse widths are 2^m times of basic one. We can see that the relative error trend to be stable when the theoretical pulse width is over 44. On the other word, when the counter frequency for pulse width is above 156.25 kHz, the relative error in quantification will not be influenced very much by counter frequency.

3.2 Temperature drift in sensors

The bias current of transistor is easily influenced by temperature, and it is usually increased with the increasing of temperature. The bias voltage of transistor is going to change with temperature. In the same reason, for the phototransistor, the bias current of it will change with temperature variation while the intensity of incident light is stable. That means the real trig voltage of phototransistor will change with temperature. With the temperature changing, the output of phototransistor will turn from 0 to 1 at different light intensity. However, the incident light intensity of phototransistor in optoelectronic position detector is determined by the relative position of the coding wheel to the window of phototransistor. If the temperature of working environment varies, position error will be introduced into the two channels of signal from two position detectors, as shown in Figure 3.

The two pulse signals A and B in Figure 3 are from the position detectors, and the two original pulse signals (solid line) which are supposed not to be disturbed by drifting are displayed. The original pulse signal is the initial pulse signal when the apparatus start to work. The width of original pulse signal represents the information of the torsion angle at the temperature that the signal is recorded. The current pulse signals (dot line) in Figure 3 are influenced by drifting. The logical relations between them are displayed in Figure 3, assuming the shadow parts ΔA and ΔB are caused by drifting and the direction of

drift is selected by random. Equation (3) shows the way to eliminate the influence of drift. After this processing, the width of current pulse signal is corrected to the original pulse width. So the output of the torque information is always the measured value in a certain temperature.

$$A\ xor\ B(org) = A\ xor\ B(cur) + A\ and\ B(cur) - A\ and\ B(org) \tag{3}$$

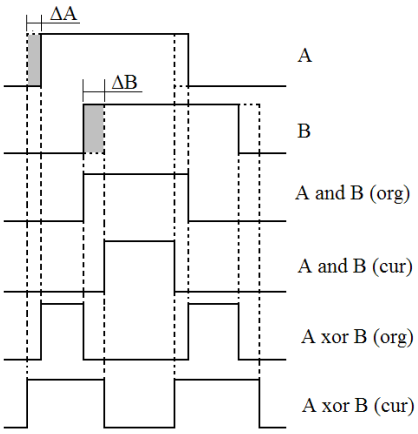

Figure 3: Diagram of temperature drift of phototransistors and signal processing

3.3 Decentred error of coding wheel

The center of coding wheel may move around the rotating axis so that the tooth in coding wheel will sway forward and backward to the optoelectronic sensor. It is called decentred error of coding wheel. There are two sources for the decentred error. The first one is caused by the torsion and deformation of shaft while the center of coding wheel and the axis of shaft coincide and the surface of coding wheel is kept perpendicular with the axis of shaft (Murawski, 2005). The decentred error won't happen in this situation if the angular speed of shaft is stable. Because the effective center angle of every sector tooth that passing through the sensitive area of sensor doesn't change, although the cross point of tooth and sensor varies.

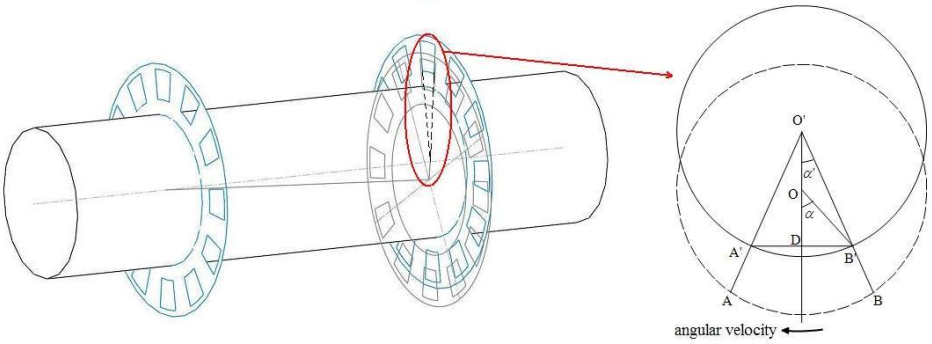

Figure 4: Diagram for decentred error of coding wheel

The other source of error is induced by the installation of coding wheel. It is caused by the problem that the center of coding wheel and axis of shaft don't coincide. As it is shown in Figure 4, the tooth is fan-shaped. When the coding wheel rotates with shaft in decentred condition, the variation of effective center angle of one tooth is shown in the right side of Figure 4. The sector A'O'B' is the original position of tooth while coding wheel center and shaft axis coincide. And AOB is the position of tooth after decentred. Because the optoelectronic sensor is fixed, the cross point of tooth and sensitive point of sensor are still at A' and B' respectively. But, currently, the real rotating center is O. It is easy to find out in Figure 4 that the angle ∠ A'OB' is bigger than the angle ∠ A'O'B'. Therefore, the effective center angle for measurement is increased when the coding wheel is mounted to make its center bias toward the axis of shaft. Vice versa, if the center of tooth bias away from the sensor, the center angle for measurement is decreased.

The angular error is calculated according to the geometry relation in Figure 4. Suppose the radiometer of shaft is R, and the angular velocity is ω, and the bias distance (OO') equals to ε. The designed center

angle of tooth is 3°, for example, so the angle α' equals to 1.5°. And the relationship of Δα and decentred distance ε and R is shown in Eq. (5). $R = O'B'$, $d = OD$, $\varepsilon = OO'$.

$$\alpha = \arctan(\frac{R\sin\alpha'}{R\cos\alpha' - \varepsilon}) \tag{4}$$

$$\Delta\alpha = \arctan(\frac{R\sin\alpha'}{R\cos\alpha' - \varepsilon}) - \alpha' \tag{5}$$

3.4 Perpendicularity error of coding wheel

Chapter 2 The perpendicularity error of coding wheel can take place in two situations. The first one is generated by the installation of coding wheel onto shaft, as shown in Figure 5. And the second one is generated by the bend of shaft while rotating. Because the optoelectronic sensors are fixed in mounting brackets, there will be a relative motion between the surface of coding wheel and optoelectronic sensor in shaft's rotating. If the measurement is done in this situation, error will be introduced to experiment data. The data in Figure 6 was the torsional angle data from Metapower system of Kongsberg Co. The experiment was done on a simulation platform for shaft running condition. The distance between them is 1 meter. In Figure 6, the x-axis is number of acquisition point, and y-axis is value of torsional angle. The vibration signal of torsional angle doesn't change with the variation of torsional angle. Its frequency is almost stable when the rotating speed is stable.

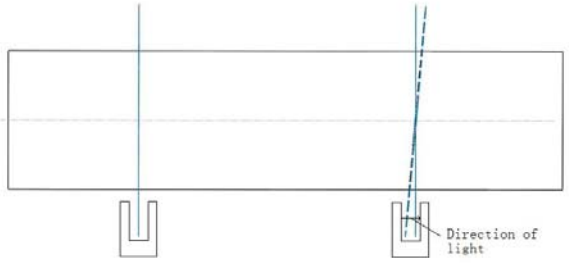

Figure 5: Diagram for the tilt of coding wheel

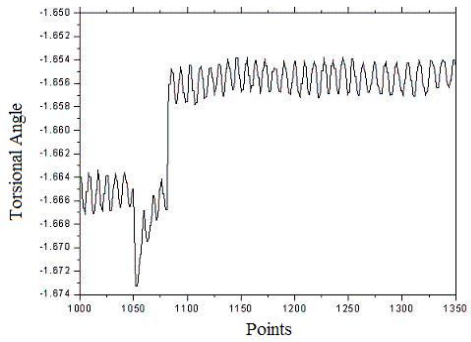

Figure 6: Vibration on torsional angle measurement

The error is calculated according to the diagram in Figure 7. The triangle AO'B is in the projective surface (perpendicular surface). It is the project of triangle AOB which is in the current surface of coding wheel. According to the sine theorem, following relationship is available as in Eq. (6). The length of AO' and BO' should be shorter than AO and BO because of projection. So the angle ∠ AO'B (θ') should be bigger than ∠ AOB (θ), which means the actual angle of sector hole for measurement is increased while the coding wheel is tilt. Suppose the central angle of the sector hole in coding wheel is 3°, and the maximum relative error is ±1 % in practical measurement, and the tilt angle of coding wheel is φ. The equivalent angle in projective surface can be described as in Eq. (6). And the allowed tilt error φ in measurement can be calculated by Eq. (7).

$$\theta' = 2\arctan\frac{\tan\frac{1}{2}\theta}{\cos\varphi} \tag{6}$$

$$\varphi = \arccos \frac{\tan \frac{1}{2}\theta}{\tan \frac{(1 \pm 1\%)}{2}\theta} \tag{7}$$

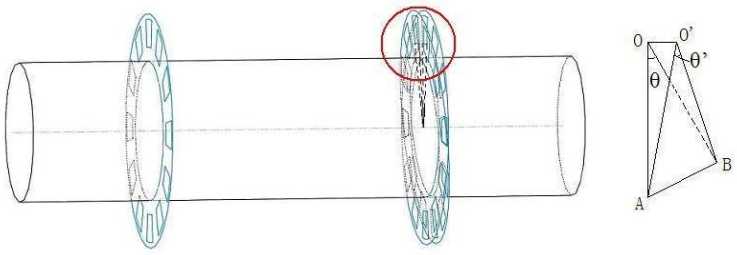

Figure 7: Diagram for variation of measurement angle

4. Conclusions

The sources of error are researched and analysed in this paper. The first one is from the quantification error in FPGA, which is caused by the counter's frequency. A 0.2816 ms width square signal is used to test the quantification error. The research result shows that the relative error is acceptable when the counting frequency is over 156.25 kHz. The second aspect of error that temperature drift in sensor is discussed in this paper. A treatment in signal processing is put forward to overcome this situation. The errors caused by inexactitude installation of coding wheels are also discussed in the research work. The decentred error and perpendicularity error are two main sources from the installation of coding wheel. The research on error tolerances of them shows that the variation of measurement angle is determined by the decentred distance and tilt angle of coding wheel. The installation requirement can be available if the range of measurement error is given according to the error tolerance equations.

References

Dai M.P. and Ji Y.Q., 2007. The Development of Axis Power Measurement System, Agricultural Equipment & Vehicle Engineering, 10, 14-17.

Drinkwater J.W., 1966. Acoustic Wire Strain Gauges, U. S. Patent 3,290,930, December 13.

Gandarillas C., 2003. Magnetoelastic Non-compliant Torque Sensor and Method of Producing Same, U. S. Patent 6,516,508 B1, February 11.

Li S.J. and Liu D.F., 2010. Research on measuring and monitoring of shaft power of naval ship. China Shiprepair, 23(5), 14-16.

Lonsdale A. and Lonsdale B., 1996. Method and Apparatus for Measuring Strain, U. S. Patent 5,585,571, December 17.

Lv Z.Y., 2008. 'The Study on Ship's Shaft Power Measurement Based Vibrating-wire Principle'. M. S. thesis, Harbin Engineering University. Harbin.

Metapower: Torque and power measurement system for rotating shafts, HSB International, 51, 54-55, 2002.

Moore J.D. and Moore E.C., 1985. Apparatus for Measuring Torque on a Rotating Shaft, U. S. Patent 4,520,681.

Murawski L., 2005. Shaft line alignment analysis taking ship construction flexibility and deformations into consideration, Marine Structures, 18, 62-84.

Yu C.B., Zhan L., Chen X.J. and Zhai F., 2005. Research on non-contact torque measurement based on screw-type differential transformer', Proceedings of the Eighth International Conference on Electrical Machines and Systems, ICEMS 2005, 3, 2366-2368.

Witte J.R., 1991. Shaft Torque Measurement, U. S. Patent 5,067,355, November 26.

Whitehead N., Jones B.E. and Rees D., 1999. Non-contact torque measurement on a rotating shaft incorporating a mechanical resonator, IEE Colloquium Innovative pressure, force and flow measurements, 10/1-10/7.

Zhu C.M., Wang Z.X. and Hu X.F., 2009. Design and study of torque measurement system, Machinery Design & Manufacture, , 30-32.